RSC Advances

ROYAL SOCIETY
OF CHEMISTRY

www.rsc.org/advances

Binary adsorption isotherms of two ionic liquids and ibuprofen on an activated carbon cloth: simulation and interpretations using a statistical and COSMO-RS models

Lotfi Sellaoui[1,2], Mohamed Bouzid[1], Laurent Duclaux[2**], Laurence Reinert[2],Salah Knani[1], Abdelmottaleb Ben Lamine[1*]

[1] Unité de Recherche de Physique Quantique, UR 11 ES 54, Faculté des Sciences de Monastir, Tunisie.

[2] Univ. Savoie Mont Blanc, LCME, F-73000 Chambéry, France.

*Correspondence to be sent to: **abdelmottaleb Ben Lamine**, Faculty of Sciences of Monastir, 5000 Monastir, TUNISIA. Email: abdelmottaleb.benlamine@gmail.com*

** *Laurent Duclaux,* Univ. Savoie Mont Blanc, LCME, F-73000 Chambéry, France. Email : laurent.duclaux@univ-savoie.fr

Abstract

The adsorption equilibriums of the binary mixtures of the 4-tert-butyl-1-propylpyridinium bromide (referred to IL1) and 4-ter-butyl-1-(2 carboxyethyl) pyridinium bromide (referred to IL2) ionic liquids and ibuprofen (2-(4-(2-methylpropyl) phenyl) propanoic acid: IBP) on activated carbon cloth were investigated. The binary adsorption isotherms of the studied systems (IL1/IL2, IL1/IBP and IL2/IBP) have been studied in different conditions (different temperatures ranging from 286 to 313 K and at various concentration ratios 0.5, 1 and 2). The experimental isotherms have been simulated by some new statistical physics models established from the grand canonical ensemble. According to the most appropriate model, the adsorbed ILs and IBP molecules are assumed to be parallel to the activated cloth surface. An inhibition effect has been observed between the adsorbed molecules. The determination of the monolayer adsorbed uptake at saturation has shown an endothermic adsorption process of IBP and an exothermic one of IL1 and IL2. The estimated energy values demonstrate a physical adsorption whatever the adsorbate species. Microscopic adsorption process was interpreted in point of view of molecular stereography and interaction energy. Moreover, the conductor-like screening model for real solvents (COSMO-RS) has been applied to calculate three specific interaction energies between the adsorbate molecules and a graphene layer modeling the activated carbon surface, i.e., the electrostatic misfit energy (E_{MF}), the hydrogen-bonding energy (E_{HB}) and the Van der Waals energy (E_{vdW}).

1- Introduction

Room temperature ionic liquids (ILs) possess an array of attractive properties such as extremely low vapor pressure, and high thermal and chemical stabilities. They are also non-flammable and high capacity solvents [1-4]. Thus, the ILs have been extensively studied as an alternative to conventional organic solvents in reaction and separation processes [4-6]. In the future, the application of ILs at an industrial scale might lead to contaminated wastewater streams. Thus the removal or recovery of ILs is an important issue to prevent their release into the environment. Among various pharmaceutical compounds, ibuprofen (IBP) is an emergent pollutant. It is detected frequently at few 100 ng up to µg concentrations in the treated sewage of the wastewater treatment plants [7].Adsorption is a low-cost separation technology that is widely used to remove the pollutants from gas and water streams. Activated carbon cloth is by far more efficient in adsorption than granulated activated carbon and powder activated carbon because of its peculiar texture enabling a direct access to the smaller pores (i.e. micropores) [8].Thus, this activated carbon type is expected to be efficient for the elimination of emergent pollutants from aqueous effluents.

Several works have reported the removal of ibuprofen from aqueous solutions by adsorption on activated carbons of different origins and physicochemical properties [8-11]. Ibuprofen was found to be adsorbed not only by dispersive interactions but also through the interaction its carboxylic group with the oxygenated groups (carbonyls and carboxyls group) of the activated carbons [12]. While ibuprofen is negatively charged at pH 7, the IL cations are positively charged and their adsorption was found to be promoted by the electrostatic attractions with the negatively charged oxygen surface groups of the carbons [13]. Palomar et al. also showed that adsorption properties of ILs at pH 7 were related both to the

hydrophobicity of the anion and the cation, depending on the alkyl chain length bonded to the cation and to the specific surface area surface of the adsorbent [14,15]. Hassan et al observed that the ultramicropores were accessible to the small ILs [16] as confirmed by Lemus et al [17]. Moreover, several studies reported that ibuprofen was adsorbed preferentially in the smaller micropores (i.e. ultramicropores) of the microporous activated carbons [18].

The aim of this work is to better understand the adsorption of binary mixture of ibuprofen and two methylimmidazolium ILs. Thus different binary adsorption isotherms of two ILs and IBP were studied at different temperatures and at various concentration ratios and further simulated. According to the literature, several methodologies have been developed to describe the binary adsorption. For example, the extended Langmuir and the extended Freundlich models provide a reasonable approach for multicomponent systems.[19-22]. The Freundlich model was developed by using an empirical approach and it refers to different parameters which did not give any pertinent information on the description of the binary adsorption [20-22]. Though it is based on a physical approach, the Langmuir model is limited to a monolayer adsorption and cannot give a complete description for the binary adsorption. In the present paper, we have developed new models based on the grand canonical ensemble in order to correlate the microscopic properties of molecules with the adsorption properties of materials. These models based on the statistical thermodynamics allow estimating parameters such as, the number of adsorbed molecules per site, the anchorage number, the receptor sites density, the saturation adsorbed uptake expression and the molar adsorption energy. From these models, the physical parameter values retrieved from the simulation enable to sketch the binary adsorption process at a molecular level if the adsorbate properties, the adsorbent porosity and surface chemistry are well known. For example, the Langmuir model assumes that one adsorption site accept one molecule; our models suppose that one receptor site can accommodate n molecules (n is an adjustable parameter). All these statistical physics models

can be developed for the general case of binary adsorption on solid of various chemical compounds in liquid or gas phase [23-25].

One disadvantage of these models is that the interactions between the adsorbate molecules are neglected. Moreover, the physical sense of the fitted parameters of the models needs to be examined carefully in relation with the system properties. The *ab-initio* molecular dynamics models (Monte Carlo simulations) of adsorption [26] allow overtaking this difficulty but they are rarely applied in liquid medium. They require a precise description of the atomic structure of the adsorbent and they are time-consuming for the calculation.

The models are used to investigate different adsorption or absorption processes such as, ionic liquids or some drugs on activated carbons, photoemissive dyes in photovoltaic devices, or absorption of hydrogen for energy storage or adsorption of odorant and gustative molecules on neuronal receptor sites. Studies of olfaction [23] and gustation [47] processes allow to get through parameters biological information in natural neurons with non-destructive methods.

In industrial painting, the knowledge of microscopic thermodynamic parameters or pertinent factors an amelioration of practical adsorption may be useful to propose experimental solutions. In photovoltaic devices (Dye sensitized solar cells: DSSCs), the aggregation of photoemissive dye molecules has a harmful effect on photovoltaic transduction performance [48]. So, the knowledge of factors, through the *n* parameter of used model or through the choice of porosimetry (PSD) of semi-conductor materials determined by our statistical physics models, allow to avoid such aggregation phenomenon. This could give directives to experimenters to try alternative new solutions. Other models were developed to describe the binary adsorption such as the 'Real Adsorbed Solution Theory' (RAST) for the liquid systems [27] and the Ideal adsorbed solution theory (IAST) [28] based on thermodynamics equations [29]. In previous works, adsorption phenomena of single adsorbates have been studied for

liquid-solid and gas-solid adsorption systems [30-32] by using the statistical physics formalism.

In this work, new statistical physics models were developed to describe the binary adsorption of two ILs and IBP on an activated carbon cloth. Moreover, the COSMO-RS (Conductor-like Screening Model for Real Solvents) model was used to evaluate the adsorption energies of ILs and IBP on a grapheme layer considered as such a model of a carbon cloth surface.

2- Experimental

2-1 Materials

2-[4-(2-Methylpropyl) phenyl] propanoic acid, also named ibuprofen (IBP) of purity higher than 98% was purchased from Sigma–Aldrich. Both ILs: 4-tert-butyl-1-propylpyridinium bromide: (IL1) and 4-ter-butyl-1-(2 carboxyethyl) pyridinium bromide: (IL2) were synthesized in our laboratory [26, 27]. An activated carbon cloth from Kuraray Chemical-Japan (Ref. 900-20) was used as adsorbent. The chemistry of surface and the porous structure of the adsorbent were studied previously [18, 42,46]. The carbon cloth (BET specific surface area of 1910 m^2 g^{-1}) was characterized by nitrogen adsorption at 77 K and carbon dioxide adsorption at 273 K. The characteristic pore volumes deduced from the DFT simulation of the N_2 and CO_2 isotherms using the slit pore model are 0.33 cm^3 g^{-1}, and 0.21 cm^3 g^{-1} for the ultramicropore (diameter < 0.7 nm), and the supermicropore (0.7 nm < diameter < 2 nm) volumes, respectively. Thus, the adsorbent is mainly ultramicroporous. The dimensions of the smaller parallelepiped volumes in which the ILs or IBP molecules are included have been calculated. These dimension values (Table 1) have taken into account the Van der Waals radius value of the hydrogen atoms (0.1 nm) at the extreme positions.

2-2 Experimental adsorption isotherm

Adsorption isotherms (at different concentration ratios and different temperatures) have been studied at pH 7.4 in phosphate buffer solutions prepared by dissolving 5.871 g of potassium dihydrogen phosphate (KH_2PO_4) and 21.512 g of disodium phosphate (Na_2HPO_4) in 5L of Ultra High Quality water (UHQ, 18.2MΩ). IL1, IL2 and IBP mother buffered solutions of given concentrations (1mmol/L for IL1/IL2 system, 1.6 mmol/L forIL2/IBP system and1.2 mmol/L for system) were used for the preparation of the binary solutions containing IL1/IL2 mixture (from 0.05 to 0.5 mmol/L) or IL2/IBP mixture (from 0.08 to 0.8 mmol/L), or IL1/IBP mixture (from 0.06 to 0.6 mmol/L). The binary isotherms were investigated at various given ratios (referred to r) of one adsorbate concentration to its coadsorbate concentration in the binary mixture. In a first step, the isotherms were studied for the three binary systems (IL1/IL2), (IL1/IBP) and (IL2/IBP) at different temperatures (T=286, 298 and 313 K) and with the same initial concentration ratios ($r = \dfrac{C_{IL_1}}{C_{IL_2}} = \dfrac{C_{IL_1}}{C_{IBP}} = \dfrac{C_{IL_2}}{C_{IBP}} = 1$). In a second step, other isotherms of the three binary systems were also studied at T=298 K and at different concentration ratios ($r = \dfrac{C_{IL_1}}{C_{IL_2}} = \dfrac{C_{IL_1}}{C_{IBP}} = \dfrac{C_{IL_2}}{C_{IBP}} = 0.5$ and 2).

Cutted disks of activated carbon cloth (about 10 mg weights) were immersed in 30 mL of the adsorbate solutions in closed flasks. They were shaked for 5 days at 250 rpm in an orbital shaker (New Brunswick Scientific, Innova 40), at three different temperatures (286, 298 and 313 K). Solutions were further filtered at 0.45 μm (Durapore®-Millipore filter). The ILs and IBP remaining concentrations were measured by higher performance liquid chromatography (HPLC) using a Waters apparatus equipped with a higher pressure pump (Waters 515), a photodiode array detector (Waters 996) and a sunfire C_{18} column (5 μm, 4.6×250 mm).). For the gradient mode analysis of IBP in mixtures with IL1 or IL2, a methanol/ultrapure water

solution (80/20, v/v), containing 0.1 vol.% of concentrated phosphoric acid (95 wt.%) was

used as a mobile phase at a flow rate of 1 mL min^{-1}.IL1 (or IL2) was also analyzed in the

same mode using a mobile phase composed of 88 % vol. (85 vol. % for IL2) of acidified

ultrapure water (1 vol. % of 95 wt.% H_3PO_4 added to the total volume) and 12 vol. % (15 vol.

% for IL2) of methanol. Detection was operated by UV absorption at 222 nm and 220 nm for

the ILs and IBP, respectively. The adsorbed amount of each adsorbate was calculated by

using the equation:

$$Q_{ads} = \frac{(C_i - C_e)}{m}V$$

(1)

where Q_{ads} is the adsorption uptake (mmol/g), V is the solution volume (L), C_i and C_e are the

initial and equilibrium concentrations (mmol/L) respectively, and m is the mass of the

activated carbon cloth (g).

3- Models for the Isotherm simulations and the calculation of the interaction energies

3-1 Theory of binary adsorption

Some assumptions are used to establish the statistical physics model expressions. In a first

hypothesis, the dissolved adsorbate molecules are treated as an ideal gas. The chemical

potential enables to describe an average interaction between the adsorbate and the adsorbant

[43]. However, the mutual interactions between the adsorbate molecules and solvent ones are

neglected.Na_1 and Na_2 variable numbers of the first adsorbate molecules and the second

adsorbate molecules, respectively, are assumed to be adsorbed onto N_M identical receptors

sites, or N_{M1} and N_{M2} receptor sites located on a unit surface of the adsorbent. All the

parameter values are given in I.S.Unities. The grand canonical partition function describing

the microscopic states of the system [33,34] is:

$$z_{gc} = \sum_{N_i = 0,1\ldots} e^{-\beta\left(-\varepsilon_i N_i - \sum_j \mu_j N_i\right)}$$

(2)

where $(-\varepsilon_i)$ is the ith receptor site adsorption energy, μ_j is the chemical potential of the jth adsorbate in the adsorption state, N_i is the receptor site occupation state, and β is defined as $1/k_B T$ (where k_B is the Boltzmann constant and T the absolute temperature). The total grand canonical partition functions can be established for identical N_M or independent N_{M1} and N_{M2} receptor sites per surface unit. For N_M identical receptor sites, it can be written:

$$Z_{gc} = \left(z_{gc}\right)^{N_M}$$

(3)

For N_{M1} and N_{M2} independent receptor sites, it can be written:

$$Z_{gc} = \left(z_{gc_1}\right)^{N_{M1}} \left(z_{gc_2}\right)^{N_{M2}}$$

(4)

The average site occupation numbers N_{oj} (j=1 or 2) can be written as:

$$N_{oj} = k_B T \frac{\partial \ln Z_{gc}}{\partial \mu_j}$$

(5)

At the thermodynamic equilibrium, the equality between the chemical potentials can be written as: $\mu_{mj} = \mu_j / n_j$ for the j adsorbate (j=1 or 2) where μ_j are the chemical potentials on the adsorption site, μ_{mj} is the chemical potential of the jth dissolved molecule and n_j the number (or fraction) per site of jth molecule.

$$\mu_{mj} = k_B T \ln\left(\frac{N_j}{z_{trj}}\right)$$

(6)

N_j represents the molecule number of the jth adsorbate, and z_{trj} is the translation partition function of the jth adsorbate of a free state [35] calculated by:

9

$$z_{trj} = V \left(\frac{2\pi m_j k_B T}{h^2} \right)^{3/2}$$

(7)

So that μ_{mj} is given by:

$$\mu_{mj} = k_B T \ln \left[\frac{c_j}{\left(\frac{2\pi m_j k_B T}{h^2} \right)^{3/2}} \right]$$

(8)

where c_j is the concentration of the jth adsorbate, m_j is the molecule mass of the jth adsorbate, h the Planck's constant and V the volume of studied system. The adsorbed amount Q_{aj} for the first or second adsorbate is written as:

$$Q_{aj} = n_j N_{Oj}$$

(9)

3-1-1 Extended Hill model (Model 1)

Two variable numbers N_{aj} (j=1 or 2) of each adsorbate are adsorbed on two independent types of receptor sites (R_j for the jth adsorbate) having N_{Mj} sites per unit of surface. The adsorption on the R_j type is achieved with the $(-\varepsilon_j)$ energy. In this model, the j type of receptor site is assumed to receive only the j type adsorbate. According to this hypothesis, the two adsorption equations must take into account the n_j stoichiometric coefficients of each dissolved molecule such as:

$$n_1 A_1 + R_1 \rightleftharpoons (A_1)_{n1} R_1$$

(10)

$$n_2 A_2 + R_2 \rightleftharpoons (A_2)_{n2} R_2$$

(11)
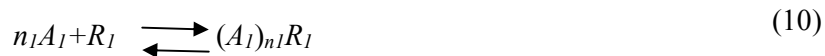
for which $n_1 \neq n_2$ in general. n_j represents the numbers of A_j adsorbate (j=1 or 2) per site, respectively. The partition function of each type of receptor site for each jth adsorbate is given in Table 2 (Equation 11).

The total grand canonical partition function is:

$$Z_{gc} = \left(z_{gc_1} \right)^{N_{M1}} \left(z_{gc_2} \right)^{N_{M2}}$$

(12)

The average number of occupied sites for each jth adsorbate is:

$$N_{0j} = k_B T \frac{\partial \ln Z_{gc}}{\partial \mu_j} = N_{M_j} k_B T \frac{\partial \ln z_{gcj}}{\partial \mu_j} = \frac{N_{M_j}}{1 + e^{-\beta(\varepsilon_j + \mu_j)}} \tag{13}$$

If $-\varepsilon_{m_j}$ ($j=1$ or 2) is the energy of the A_j adsorbed molecule at equilibrium, it can be written

$$\varepsilon_{mj} = \varepsilon_j / n_j. \tag{14}$$

The number of occupied sites for the jth adsorbate becomes:

$$N_{0j} = \frac{N_{M_j}}{1 + (e^{-\beta(\varepsilon_{mj} + \mu_{mj})})^{nj}} = \frac{N_{M_j}}{1 + (e^{-\beta\varepsilon_{mj}})^{n_j} (\frac{z_{trj}}{N_j})^{nj}} \tag{15}$$

where z_{trj} is the partition function of translation corresponding to the jth adsorbate. At the

concentration: $(c_{1/2})_j = z_{v_j} e^{-\beta\varepsilon_{mj}}$, the respective number for the jth adsorbate of the

occupied sites is the half of the total number of the receptor sites for the jth adsorbate ($N_{0j} = N_{Mj}/2$) and thus:

$$N_{0j} = \frac{N_{M_j}}{1 + \left(\frac{(c_{1/2})_j}{c_j}\right)^{n_j}} \tag{16}$$

where c_j represents the concentration in solution of jth adsorbate and $c_j = N_j/V$.

The number of the jth adsorbed molecules versus concentration given in Table 2 (equation 17) expressed from equation (9) where $(c_{1/2})_j$ is the concentration at half saturation for the jth type of receptor site.

3-1-2 Extended Langmuir model (Model 2)

This model is a particular case of model 1, in which $n_1 = n_2 = 1$. Based on the equation (17) of the first model, the adsorbed quantity of the jth type of molecule as a function of c_j

concentration (c_j is the concentration in solution of the jth adsorbate) is given by equation (18) mentioned in Table 2.

3-1-3 Exclusive extended Hill model (Model 3)

In this model, the molecules are supposed to be adsorbed on only one type of receptor sites (R type) with the N_M density. However, the R type receptor sites could receive exclusively the A_j ($j=1$ or $j=2$) molecules with the energies $(-\varepsilon_j)$. The value of n_1 is assumed to be different fromthe one of n_2 ($n_1 \neq n_2$). In this case, the adsorption equations for the A_j molecule of adsorbate are given by:

$$n_1 A_1 + R \; \rightleftharpoons \; (A_1)_{n1} R \qquad (19)$$

$$n_2 A_2 + R \; \rightleftharpoons \; (A_2)_{n2} R \qquad (20)$$

The partition function of one receptor site (with three different states of a site: empty, occupied by A_1 or occupied by A_2) is written in Table 2 (equation 21), where μ_1 and μ_2 are the chemical potentials of the A_j ($j=1$ or $j=2$) molecule of adsorbate on the R site.

The total grand partition canonical function is calculated using the relation (3).The same calculations described in the section 3.1 have allowed obtaining the expression of the number of A_j type adsorbed molecules from equation (9).

Finally, the adsorbed quantity for the jth adsorbate as a function of the concentrations is calculated from equation (22) in Table 2, where c_{01} and c_{02} represent the concentrations at half saturation of the first and second adsorbate, respectively and the $Q_{asatj}=n_j N_M$ quantity represents the monolayer adsorbed quantity for the jth adsorbate (Aj molecule).

3-1-4 Extended Langmuir model (model 4)

In this model, the particular $n_1=n_2=1$relationis assumed which leads to an extended Langmuir equation. The equation (22) becomes then equation (23) inTable 2.

3-1-5 Non–exclusive extended Hill model (Model 5)

The molecules are assumed to be adsorbed on one type of receptor site (R) having the N_M density which can receive either A_1 or A_2 or both A_1 and A_2. According to this hypothesis the adsorption equation is given by:

$$2n_1A_1 + 2n_2A_2 + 3R \quad \rightleftharpoons \quad (A_1)_{n1}R + (A_2)_{n2}R + (A_1)_{n1}(A_2)_{n2}R \qquad (24)$$
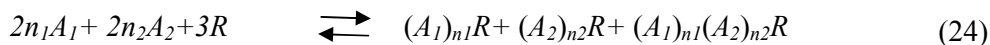
The partition function of one receptor site is given in Table 2 (equation 25).The total partition function can be calculated from equation (3).The adsorbed amount as a function of different concentrations c_1 and c_2,given in Table 2 (equation 26) where c_{01} and c_{02} represent the concentrations at half saturation), is calculated using equation (9) and (5) from the number of adsorbed molecules of the jth adsorbate derived from the total partition function.

3-1-6 Non exclusive extended Langmuir model (model 6)

For $n_1=n_2=1$, the adsorbed quantity of the jth adsorbate calculated from model 5 is written as equation (27) given in Table 2.Table 2 shows the partition function and the adsorbed quantity for each model.

3-2 Simulations of the isotherms by the statistical physics models

The binary experimental isotherms at different temperatures and at different concentrations ratioswere simulated by using the six statistical physics models previously established in section 3-1. Many other models could have obviously been considered but our simulations were limited to these six proposed models. Five parameters have been adjusted by the numerical simulations: the numbers of molecules per site (n_1, n_2), the density of receptor sites (N_M) and the concentrations at half saturation (c_{01}, c_{02}). The fitting mathematical method is based on the Levenberg-Marquardt iterating algorithm using a multivariable non-linear regression. The best fitting result is established once the residuals between the experimental data and values predicted by the model are minimized according to a 95% confidence level [36,37]. The R^2 multiple correlation squared (coefficient of determination) and the $RMSE$ residual root mean square error (i. e. the estimated standard error of the regression) have

beendetermined. The model has been considered as correct and the parameter estimates unbiased, while approximately 95% of the estimated adsorbed amount has had to fall within ±2 *RMSE* of their true values. For a p number of adjustable parameters the estimated standard error is given by [36,37]:

$$RMSE = \sqrt{\frac{RSS}{m'-p}}$$

where *RSS* is the residual sum of squares: $RSS = \sum_{j=1}^{m'} (Q_{jcal} - Q_{j\exp})^2$, and where Q_{jcal} and Q_{jexp} are calculated and experimental values of adsorbed quantity respectively, and *m'* is the number of experimental data.

3-3 Calculation of the interaction energies using COSMO-RS model

The interaction energies of the three adsorbates with the adsorbent (activated carbon cloth) were estimated by using the COnductor-like Screening MOdel for Real Solvents (COSMO-RS model). This model allows calculating several thermo-physical properties from the geometric coordinates of all the individual atoms. The COSMO-RS model [42] combines quantum chemical approaches, based on the dielectric continuum model known as COSMO, with statistical thermodynamics calculations. In the COSMO calculations, the molecules are surrounded by a virtual conductor environment, and the interactions are considered to take place on segments of this perfect/ideal conductor interface [38-41] taking into account the electrostatic screening and the back-polarization of the solute molecule. Thus, the discrete surface around the solute molecule and each segment is characterized by their geometry and the (σ) screening charge density at a minimum energetic state of the conductor. The complete description of the molecule is achieved by a distribution function designed by σ-profile $p_s(\sigma)$ that describes molecular interactions [41]. Additionally, COSMO-RS considers three specific interaction

energies (three specific interaction energies of a molecule with its environment), described as a function of the polarization charges of the two interacting segments - (σ, σ') or $(\sigma_{acceptor}, \sigma_{donor})$:

- ✓ Electrostatic misfit interaction: $E_{MF}(\sigma, \sigma')=a_{eff}\alpha'/2(\sigma, \sigma')^2$,   (28)

- ✓ Hydrogen -bonding energy: $E_{HB}=a_{eff}c_{HB}min(0; min (0, \sigma_{donor} + \sigma_{HB})\times max(0; \sigma_{acceptor} - \sigma_{HB}))$,   (29)

- ✓ Van der Waals energy: $E_{vdW}=a_{eff}(\tau_{vdW}+\tau'_{vdW})$,   (30)

where a_{eff} is the effective contact area between two surface segments, α' is an interaction parameter, c_{HB} is the hydrogen-bond strength, (σ_{HB}) is the threshold for hydrogen-bonding, and τ_{vdW} and τ'_{vdW} aresome element specific Van der Waals interaction parameters. The total interaction energy is given by: $E_T= E_{MF} + E_{HB} + E_{vdW}$.

The structure of activated carbons is known to be formed of randomly oriented nanometer-sized graphene planes (model of "crumpled paper") [45], thus the adsorbent was assumed to be chemically an arrangement of graphene layers with only hydrogen atoms bonded at the edge of the planesand the adsorbent surface was modeled by a graphene plane (44 atoms of Carbon and 20 atoms of Hydrogen at the edges of the layer) with a limited in-plane extension (Figure 1). This was assumed as a fluid phase interacting with the adsorbates binary mixtures (IL1/IL2 orIL1/IBPorIL2/IBP) in order to estimate the interaction energies via a COSMO-RS model. The atomic coordinates of each studied adsorbate (IL1, IL2 and IBP) have been estimated using the Chemsketch software from the developed formulas mentioned in Table 1. Thus the $p_s(\sigma)$ σ- profile of the adsorbates and the grapheme have been determined through Turbomole. For the quantum method parameterization, the BP_TZVP_C21_0110 (Triple-ζ valence polarized quantum chemical method) was used for the calculation of the physicochemical data (i.e. functional and basic sets). The different specific energies of

interaction between the two adsorbates (IL1/IL2 or IL1/IBP or IL2/IBP) and the activated carbon cloth surface (the adsorbent) have been calculated.

In our work, the COSMO-RS model has been used to calculate the interaction energy of one molecule interacting with its environment, which is in fact a mixture of adsorbates, and adsorbent without taking into account of the solvent (i.e. the water). The energies of interaction of the first adsorbate or the second adsorbate with their environment (mainly formed of the graphene plane), have been calculated at 298 K for some given molar fractions values determined from the experimental data obtained at saturation. The calculation of the interaction energies with the graphene surface has been determined at a molar fraction of each adsorbate molecule equal to 0.2273.

4- Results and Interpretations

4-1 Simulation results and interpretation of the binary adsorption isotherms

4-1-1 Determination of the best simulation model

The R^2 and the$RMSE$ values of the simulated isotherms (at different temperatures and at r=1) are reported in Tables 3 and 4, respectively.

The values of the R^2 determination coefficients of the three studied systems (at T=298 K and at r=0.5 and 2) calculated by using the model 3 vary between 0.988 and 0.997. According to the Tables 4 (R^2 values) and 5($RMSE$ values), and the R^2 values for the three studied systems at T=298 K and at r=0.5 and 2, the model 3 shows the highest R^2 and the lowest $RMSE$ values compared to the other models. Thus, the binary adsorption process of the three studied systems in our different experimental conditions is better described by model 3. The profile of the simulated different adsorption isotherms at different temperatures (and at r=1) are shown

16

in Figure 2. The simulated binary adsorption isotherms at T=298 K, and at r=0.5, 1 and 2 are reported in Figures 3, 4 and 5, respectively.

The adsorption capacities at r=1 (Figures 3, 4 and 5) are found in the following order: IBP>IL1>IL2. The adsorbate molecules possess all quite similar volume. Thus, whatever the adsorbate molecule, almost the same proportion of micropore volume of the carbon cloth is accessible to the adsorbate. Thus, no effect of sizing of the molecules could explain the difference found in the adsorption capacities. All the adsorption isotherms of IBP show a "Langmuir" shape with a pronounced knee and a plateau. Moreover, the adsorption isotherms of IBP exhibit higher adsorption uptakes at low concentrations than the ones of IL1 and IL2. This means that at low concentration IBP is interacting with thecarbon surface at higher energy value than the two ILs. This could be also related to the solubilities. Though the molecule of IBP is dissociated (negatively charge molecule) at the working pH (pH=7.4), its solubilityis limited (about 107 ppm) due to its hydrophobic character. By contrast, the ILs (IL1 and IL2) are more soluble than IBP (soluble in the studied concentration domain). Thus, in comparison with the ILs, the adsorption of IBP is promoted by its hydrophobic nature in relation with its highest K_{ow} (octanol/water partition coefficient) value compared to IL1 and IL2 (Table 1). For r=1 (equimolar concentration), the adsorption uptake of one adsorbate with respect to its coadsorbate are in agreement with the K_{ow} value of each molecule: the greater the hydrophobicity, the higher the uptake.

4-1-2 Thermal evolutions of the numbers of molecules per site (n_j), the densities of receptor sites (N_{Mj}) and the monolayer adsorbed uptakes ($Q_{asat\,j}$)

> **n_1 and n_2**

The n_1 and n_2 stoichiometric coefficient values representing the numbers of molecules per site of the jth adsorbate are average numbers (integer number in case of one site), which can be

greater or smaller than the unity. A n_j greater than 1, represents the number of docked molecules per site, according to a multimolecular adsorption mechanism [25, 36]. If this value is smaller than 1, $1/n_j$ represents the anchorage number of one molecule on several different receptor sites [25, 36]. Generally $1/n_j$ (j=1,2) represents an average value of many anchorage numbers. Assuming an average of two anchorage values characterized by two $n$integer values (number of molecule per site), one can calculate the proportion among the sites of each anchorage type. For example, the IL1 ionic liquid n_j value in IL1/IBP mixture is 0.57 at T=286 K, which can be considered as an average between 1/2 and 1.The relation $0.57 = x \times 1 + (1 - x) \times 0.5$ enables to calculate the percentage values of single docked molecule *(x=14%)* and double docked one (1-*x*=86%).

All the values of the IL1, IL2 and IBP molecules numbersper siteat r=1are less than 1 at the studied temperatures and are in same order of magnitude (Figure 6). This indicates a multi-docking of the adsorbed molecules which might be docked parallel to the activated carbon surface. The n_j values of IL1/IL2 and IL2/IBP systems are nearly constant with temperature and variesin the opposite sense. For example, if n_1 of IL1 increases, n_2 of IL2 decreases. This suggests an inhibition effect between the two kinds of adsorbates on the same receptor site for the IL1/IL2 and IL2/IBP studied systems. This would mean that the adsorption of one adsorbate excludes partly the other. This could berelated tosimilar steric nature of interactions between adsorbent and adsorbate (IL1 and IL2, or IL2 and IBP) which could occupy the same sites.

As a conclusion, for the IL1/IL2 and IL2/IBP binary systems, (n_1+n_2) value remains constant versus temperature as one adsorbate could replace the other because the IL1 and IL2 or IL2 and IBP molecules probably occupy the same kind of site.

However, for the IL1/IBP system, the n_1 and n_2 values decrease togetherwith temperature under the influence ofthermal agitation.   The molecules were not mutually excluded

indicating that the two molecules might occupy different types of sites. For the IL1/IBP system, the thermal agitation has acted the same way on the two molecules.

> ➤ **N_{M1} and N_{M2}**

All the N_{Mj} variations *versus* temperature (Figure 7) are in agreement with the n_1 and n_2 variations (Figure 6). Indeed, the N_{Mj} variation for each adsorbate of all binary system is always in the opposite sense of the corresponding n_j variation. This could be due to a steric hindrance hiding some neighbor receptor sites as n_j value is increased.

Thus, IL1 and IL2 in one hand and IL2 and IBP in the other hand could occupy the same sitesbut their adsorption energies were found different, respectively (Figure 9).For the IL1/IBP system, the adsorbates occupy different sites.

> ➤ **Q_{asat1} and Q_{asat2}**

The value of Q_{asatj} (part 3.1.3), depends both on n_j and N_{Mj}. The monolayer adsorbed capacities follow two kinds of temperature dependenceas increasing the temperature (Figure 8): (i) for (IL1/IL2) system, a decrease in the monolayer adsorbed uptake for both IL1 and IL2, while (ii) for (IBP/IL1) and (IBP/IL2) systems an increase in theIBP uptake and a constant variation for both IL1 and IL2. The decreasing uptake as heating is related to the exothermic adsorptions of IL1 and IL2, but the increasing oneis due to the endothermic adsorption of IBP in agreement with the adsorption energies displayed in Figure 9. According to the profile of the T=298 K isotherms at different concentration ratios (r=0.5, 1 and 2) (Figure 2, 3 and 4), the saturation uptake of an adsorbate increases while rising its ratio.

4-2 Adsorption energies

4-2-3 Adsorption energies from the isotherm fitting

The adsorption energies ($-\varepsilon_j$) characterizing the interactions between each adsorbate (ILs or IBP) and the adsorbent (activated carbon cloth) have been determined from equation (31) [42]. The c_{0j} concentrations at half saturation are related to the temperature (T), the solubilities of the adsorbates (s_j), and the adsorption energies ($-\varepsilon_j$):

$$c_{0j} = s_j \times \exp(-\varepsilon_j / RT) \tag{31}$$

The adsorption energies and the solubility values were calculated from the c_{0j} values obtained by the adsorption isotherms fitting at the three temperatures. The s_j and ε_j values were refined by the fitting of the c_{0j} values at the three temperatures.

The interaction energies values (Figure 9) are lower than 40 kJ/mol demonstrating that the various adsorbates interact through a physical adsorption with the activated carbon surface (Van Der Waals interactions and/or hydrogen binding)[42]. The ILs adsorption energies are always negative corresponding to an exothermic adsorption (Figure 9). By contrast, they are positive for the adsorption of IBP indicating an endothermic process.

The endothermic adsorption of IBP was also reported by different authors in water [44]. This endothermic adsorption could be driven by an increase in entropy. As a matter of fact, the endothermic nature of adsorption of IBP in the high concentration range (0.08 to 0.8 mmol/L with IL2 and 0.06 to 0.6 mmol/L with IL1) could be explained by the release of water molecules concomitant to the IBP adsorption. Indeed, the IBP molecules could compete with the solvent (water) for some adsorption sites or the molecules could de-solvate through their adsorption process.

4-2-1 COSMO-RS predictions of the interaction energies

Table 5 reports the interaction energies calculated numerically by COSMO-RS describing the interaction between each adsorbate and the adsorbent in each binary system in the absence of water. The calculations were realized at given molar fractions of the adsorbate1/adsorbate2/adsorbent system: 0.2273 0.2273 0.5455. According to Table 5, the attractive Van der Waals interaction (VdW) has played the main role in the adsorption of the three adsorbates. For IL2 and IBP, the hydrogen- bonding (H-B) has played the second role and the misfit electrostatic interaction (referred to misfit) has had a negligible effect. On the contrary, for the adsorption of IL1, the misfit interaction has played the second role but the hydrogen- bonding has had no effect. The differences in these interaction energies are probably related to the molecular structure of the adsorbate molecules. Indeed, IL2 and IBP contain a carboxyl group which contributes to the adsorption in term of hydrogen-bond interaction. Thus, the total interaction energy from COSMO-RS calculation (sum of the electrostatic interaction, hydrogen bond contribution and Van der Waals contribution) of IL2 is higher than the one of IL1 in agreement with the adsorption energies obtained from the isotherms simulations. This is due to the contribution of the hydrogen bond interaction related to the carboxyl functional group which is only present in IL2. The value of interaction energies obtained by COSMO-RS calculations (i. e. about -50 kJ/mol for IL1, about -68 to -70 kJ/mol for IL2 and about -60 to -61kJ/mol for IBP) are ten times the ones obtained by the simulation of the isotherms. This is because the COSMO-RS model has allowed calculating interaction energy on a nude carbon surface without any solvent interaction which could rather correspond to the energy of interaction for the first sites of adsorption at very low concentration. As a difference, the simulation of the isotherms enables to determineaglobal interaction energy for the high concentration range.

Moreover, the COSMO-RS model cannot take into account: (i) the interaction with water that makes endothermic the IPB adsorption process, and (ii) the hydrophobicity of IBP that allows

its higher uptake compared to IL1 and IL2. The values of the fugacities calculated from the COSMO-RS model in the mixture, are not exactly in agreement with the adsorption uptake on the carbon surface (see supplementary information) because the COSMO-RS model does not allow simulating the adsorption phenomenon.

5- Conclusion

Using the grand canonical ensemble in statistical physics, different models for the binary adsorption systemshave been developed. Among the proposed models, theexclusive extended Hill model (model 3) better reproduces the different adsorption isotherms at different temperatures and at different concentration ratios. According to this adequate model, the ILs and IBP are supposed to be adsorbed on two sites (double docked) on the activated cloth surface. An inhibition effect (competition) has been observed between the adsorbed molecules of ILs and IBP but not between the two ILs molecules. The adsorption uptake of IBP is always higher than the one of ILs due to its hydrophobic nature. The adsorption process is found exothermic for the ILs but endothermic for IBP possibly because of its interaction with solvent (water). Simulations using the COSMO-RS model show that the attractive Van der Waals interaction plays a main role in the adsorption of all the adsorbates. The calculation of the adsorption energies has demonstrated the contribution of hydrogen-bond interaction for IL2 due to the presence of a carboxylic group in this molecule in agreement with its higher uptake than IL1. This has suggested that IL2 and IBP could compete for adsorption on some sites both through Van der Waals and/or hydrogen bond interactions, while IL1 and IBP could compete only for adsorption on sites controlled by Van der Waals interactions.

References

[1] T. Welton,Chem. Rev., 1999, 99, 2071.

[2] P. Wasserscheid and T. Welton, Ionic liquids in synthesis,Weinheim: Wiley-VCH; 2008. p. 175–261.

[3] R.D. Rogers, K.R. Seddon., American Chemical Society; 2003.

[4]R.D. Rogers, K.R. SeddonandS.Volkov, Green Industrial Applications of Ionic Liquids, first ed Springer, 2003.

[5] R.D, Rogers, K.R, Seddon.,American Chemical Society 2005.

[6] X. Han, D.W, Armstrong, Ionic liquids in separations, AccChem Res 2007, 40, 1079.

[7] K. Fent, A. Weston, Aquat Toxicol., 2006,76, 122.

[8]E. Ayranci, N. Hoda, Chemosphere.,2005, 60, 1600.

[9] A.S.Mestre, A.S.Bexiga, M.Proenca, M. Andrade, M.L.Pinto, I.Matos, I.M.Fonseca, and A.P.Carvalho, Bioresour.Technol., 2011, 102, 8253.

[10] A. S. Mestre, J. Pires, J.M.F. Nogueira, J. B. Parra, P.A. Carvalho and C.O. Ania, Bioresource Technology., 2009, 100,1720.

[11] S.P.Dubey, A.D. Dwivedi, M. Sillanpääa and K.Gopal, Chem. Eng. J., 2010, 165, 537.

[12] H. Guedidi, L. Reinert, J.M. Lévêque, Y. Soneda, N. Bellakhal and L. Duclaux, Carbon., 2013, 54, 443.

[13] A. Farooq, L. Reinert, J.M. Leveque, N. Papaiconomou, N. Irfan and L. Duclaux, MicroporousMesoporous Mater., 2012,158, 55.

[14] J. Palomar, J. Lemus, M.A. Gilarranz and J.J. Rodriguez,Carbon., 2009, 47, 1846.

[15] A.B. Pereiro, J.L. Legido and A. Rodriguez, J. Chem. Thermodyn., 2007,39, 1168–1175.

[16] S.Hassan, L. Duclaux, J. M. Leveque, L. Reinert ,A. Farooq and T.Yasin, Journal of Environmental Management., 2014, 144, 108.

[17] J. Lemus, J. Palomar , F. Heras, M.A. Gilarranz and J.J Rodriguez,, Sep. Purif. Technol., 2012, 97, 11.

[18]H. Guedidi, L. Reinert, Y. Soneda , N. Bellakhaland L. Duclaux,Arabian Journal of Chemistry (2014)http://dx.doi.org/10.1016/j.arabjc.2014.03.007.

[19] L. Foong, K. Fung, J. BarfordaandG. McKay, Journal of Colloid and Interface Science., 2013, 395, 230.

[20] E.A. James, D.D. Do, J. Chromatogr. 542 (1991) 19.

[21] K.H. Chu, J. Hazard. Mater.B90 (2002) 77.

[22] C. Sheindorf, M. Rebhun, M. Sheintuch, J. Colloid Interface Sci. 79 (1) (1981) 136.

[23] A. Ben Lamine, Y. Bouazra, Chem. Senses., 1997, 22, 67.

[24] M. Khalfaoui, A. Nakhli, Ch. Aguir, A. Omri, M. F. M'henni and A. Ben Lamine, Environ Sci. Pollut. Res., 2014, 21,3134.

[25] L. Sellaoui, S. Knani, A. Erto, M. A. Hachicha and A. Ben Lamine, Fluid Phase Equilibria, 2016, 408,259.

[26] J.Puibasset, R. J. M. Pellenq, Studies in Surface Science and Catalysis, 2007, 535.

[27] A. Erto A. Lancia and D. Musmarra,Microporous and Mesoporous Materials., 2012, 154 45.

[28]A. Erto , A. Lancia and D. Musmarra, Separation and Purification Technology., 2011, 80 140.

[29] A.Vishnoi ,T.Banerjee, P.Ghosh , Sk. Musharaf Ali , K.T.Shenoy, Separation and Purification Technology., 2014, 133,138.(fausse reference)

[30] M. Khalfaoui, M.H.V. Baouab, R. Gauthier and A.B. Lamine, Adsorpt. Sci. Technol., 2002, 20, 17.

[31] M. Khalfaoui, S. Knani, M.A. Hachicha, and A. Ben Lamine, Journal of Colloid and Interface Science., 2003, 263, 350.

[32] S. Knani,, F. Aouaini , N. Bahloul , M. Khalfaoui , M.A. Hachicha , A. Ben Lamine and N. Kechaou, Physica A., 2014, 400,57. 400.

[33] M. Khalfaoui, A. El Ghali, C. Aguir , Z. Mohamed, M. H. Baouab and A Ben Lamine. Industrial Crops and Products., 2015,67,169.

[34] Y. Ben Torkia, M. Ben Yahia, M. Khalfaoui ,S.A. Al Muhtaseb andA. Ben Lamine Physica B., 2014, 433,55.

[35] M. Ben Yahia, S. Knani, H. Dhaou, M.A. Hachicha, A. Jemni, A. Ben Lamine Int. J. Hydrogen Energy., 2013, 38,536.

[36] L. Sellaoui, H. Guedidi, S. Knani, L. Reinert, L. Duclaux and A.Ben Lamine, Fluid Phase Equilibria., 2015,103.

[37] D.G. Kinniburgh, J.A. Barker and M.A. Whitfield, J. Colloid Interface Sci.,1983, 95,370.

[38] A. Klamt, F. Eckert, Fluid Phase Equilibria., 2000,172,43.

[39] M. Diedenhofen, A. Klamt, Fluid Phase Equilibria., 2010, 294,31.

 [40] A, Klamt, F. Eckert and w. Arlt, Annu Rev,Chem Biomol Eng., 2010, 1, 101.

[41] A. Klamt, Amsterdam Elsevier (2005).

[42] L. Sellaoui, H. Guedidi, S. Masson, L. Reinert, J.-M.Levêque, S. Knani, A. Ben Lamine, M. Khalfaoui and L. Duclaux, Fluid Phase Equilibria., 2016, 414,156.

[43] C. Chahine, P.Devaux, Thermdynamique statistique,Dunod, Paris 1976.

[44] S. Álvarez- Torrellas, A. Rodríguez, G. Ovejero, J. García, Chemical Engineering Journal., 2016, 283,936.

 [45] J.N. Rouzaud, A. Oberlin., Carbon., 1989, 27, 517.

[46] H. Guedidi Ben Slama, Ph. D thesis, Preparation and modification of activated carbons for adsorption of the emerging organic pollutants (pharmaceutical molecules and ionic liquids), University Savoie Mont-Blanc, 2015.

[47] S. Knani, M. Mathlouthi, A. Ben Lamine, Food Biophys. 2007,2 183.

[48] S. Kambe, K. Mursakoshi, T. Kitamura, Y. Wada, S. Yanagida, H. Kominami, Y Kera, Sol Energy Mater. Sol Cells. 2000, 61, 427.

Figure 1: Molecular model for the activated carbon cloth surface.
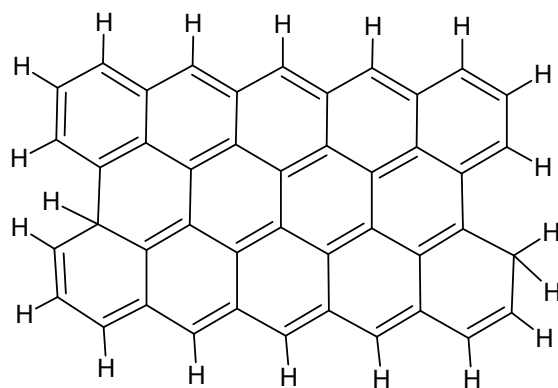
Figure 2: *The adsorption isotherms at different temperatures and at r=1: (a: IL1/IL2, b: IL2/IBP, c: IL1/IBP). The experimental points are represented by symbols and the continuous lines are the fitted isotherms using the model 3.*
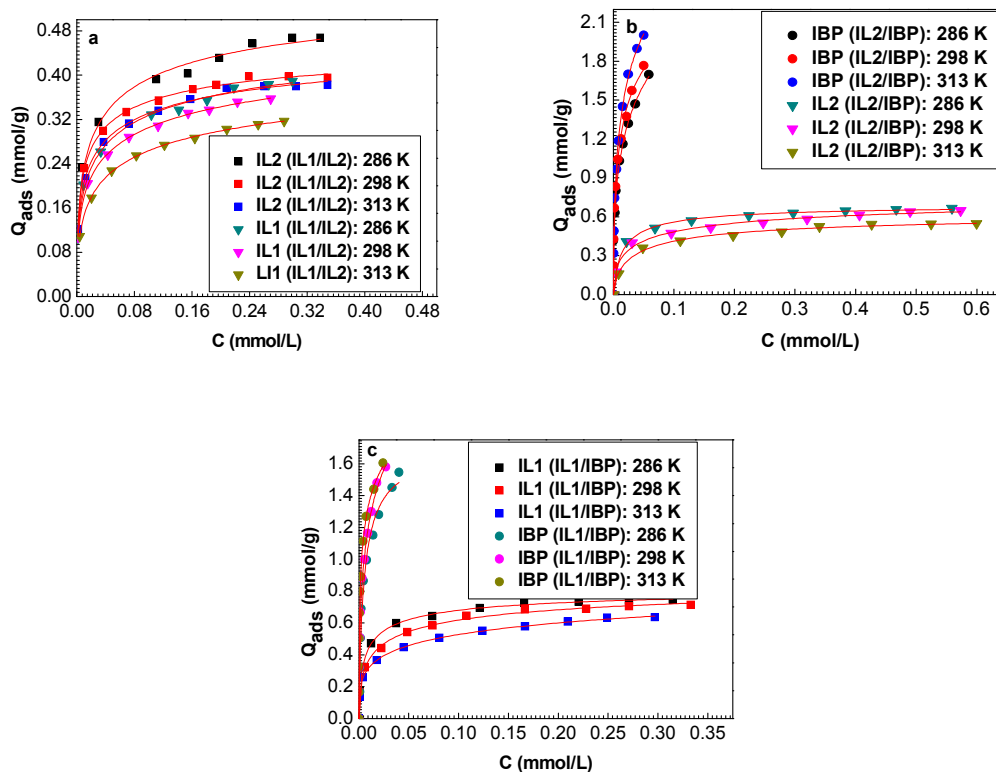
Figure 3: *The adsorption isotherms at only T=298 K and at different concentration ratios for the studied system IL1/IL2. The experimental points are represented by symbols and the continuous lines are the fitted isotherms using the model 3.*
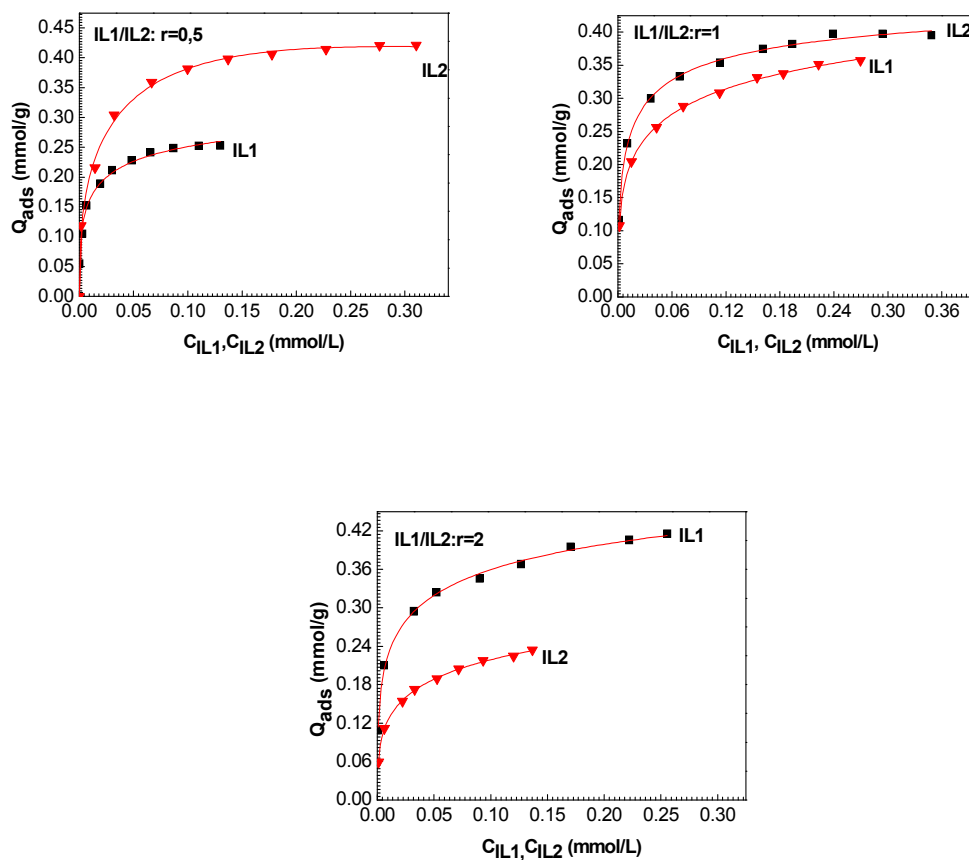
Figure 4: *The adsorption isotherms at only T=298 K and at different concentration ratios for the studied system IL1/IBP. The experimental points are represented by symbols and the continuous lines are the fitted isotherms using the model 3.*
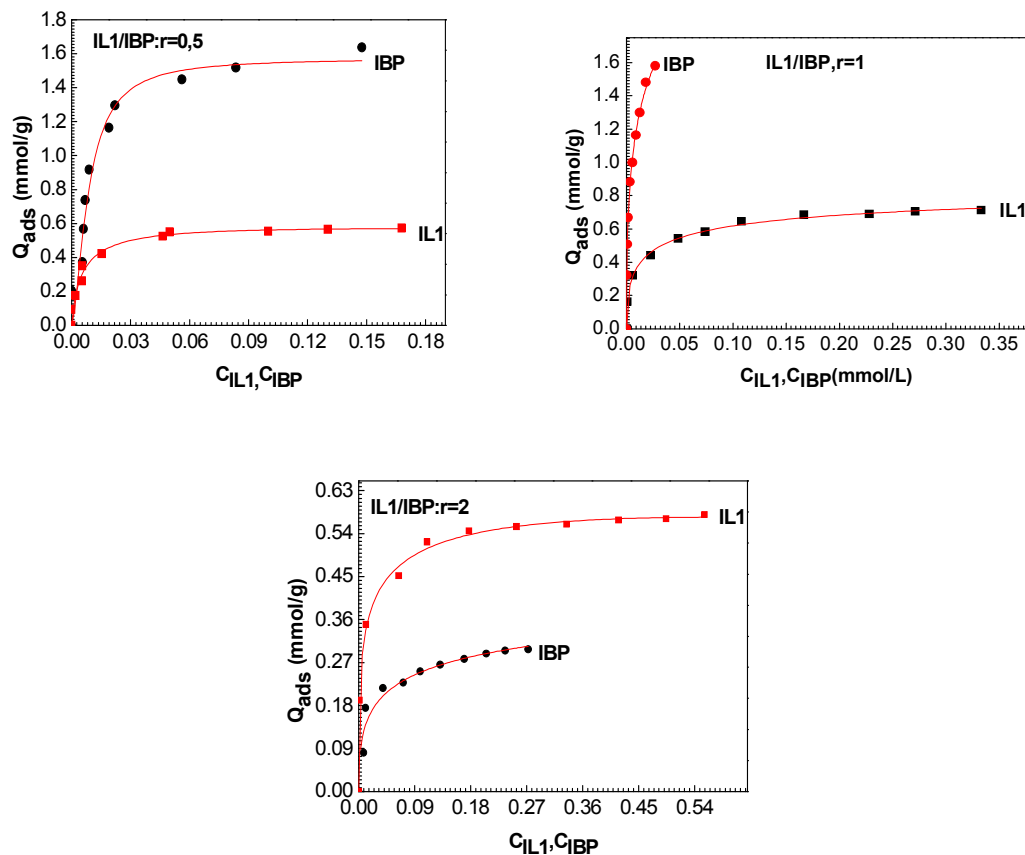
Figure 5: *The adsorption isotherms at only T=298 K and at different concentration ratios for the studied system IL2/IBP. The experimental points are represented by symbols and the continuous lines are the fitted isotherms using the model 3.*
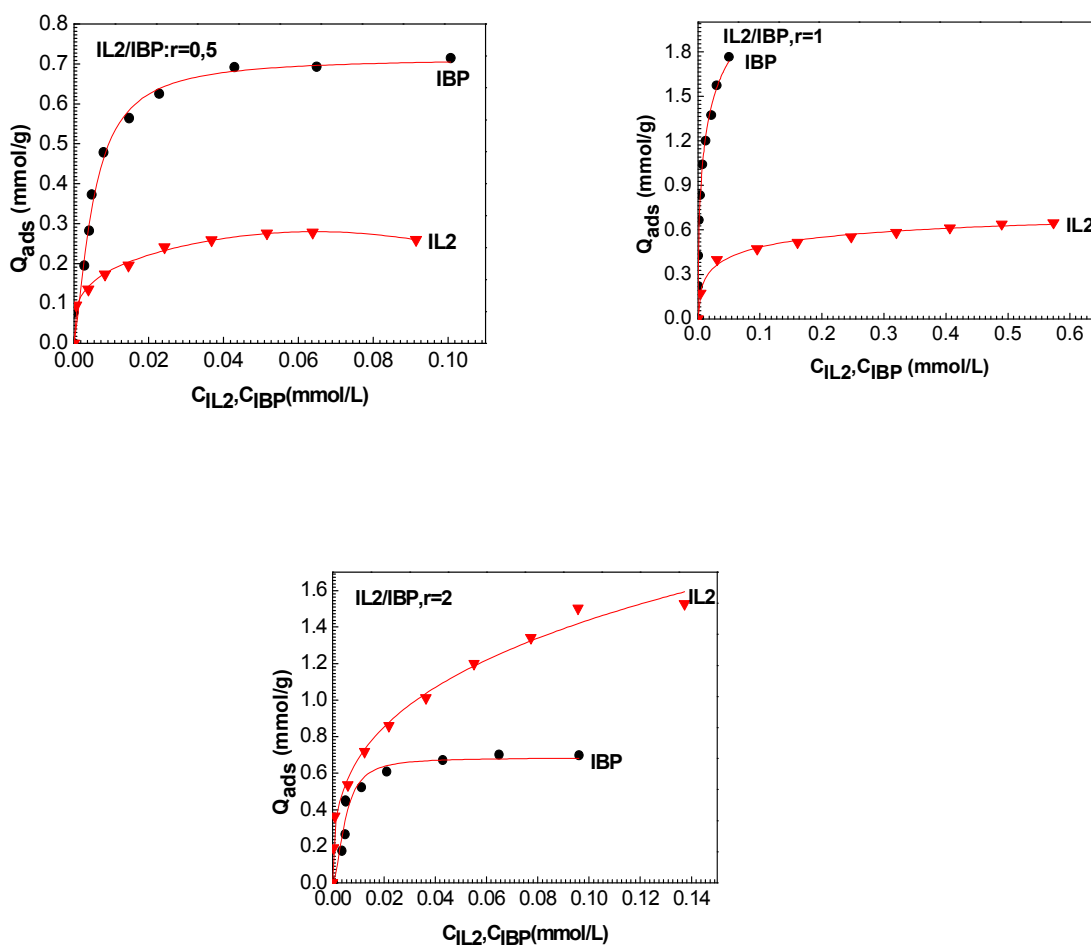
Figure 6: *Evolution with temperature of the numbers of molecules per site n₁ and n₂ for the three studied binary systems at r=1.*
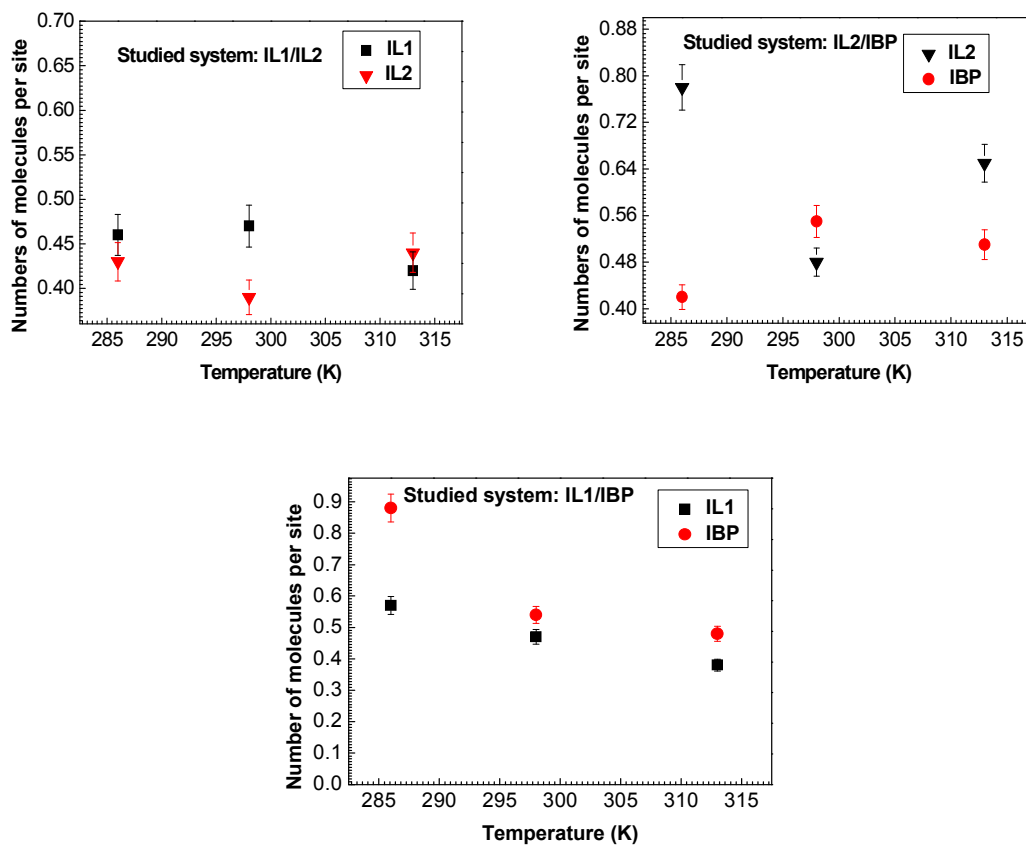
Figure 7: Temperature dependence of the density of receptor sites N_{M1} and N_{M2} for the three studied systems at r=1.
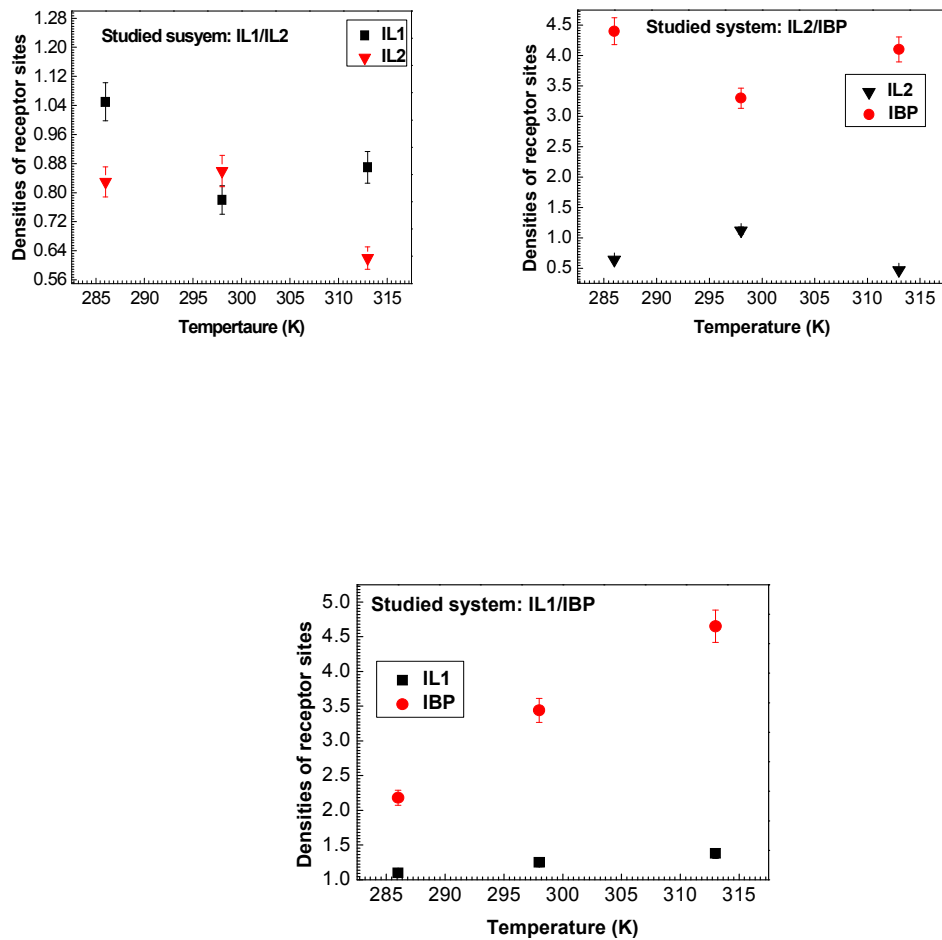
Figure 8: *Evolution of the monolayer adsorbed uptake versus temperature for the three*

studied binary systems (r=1).
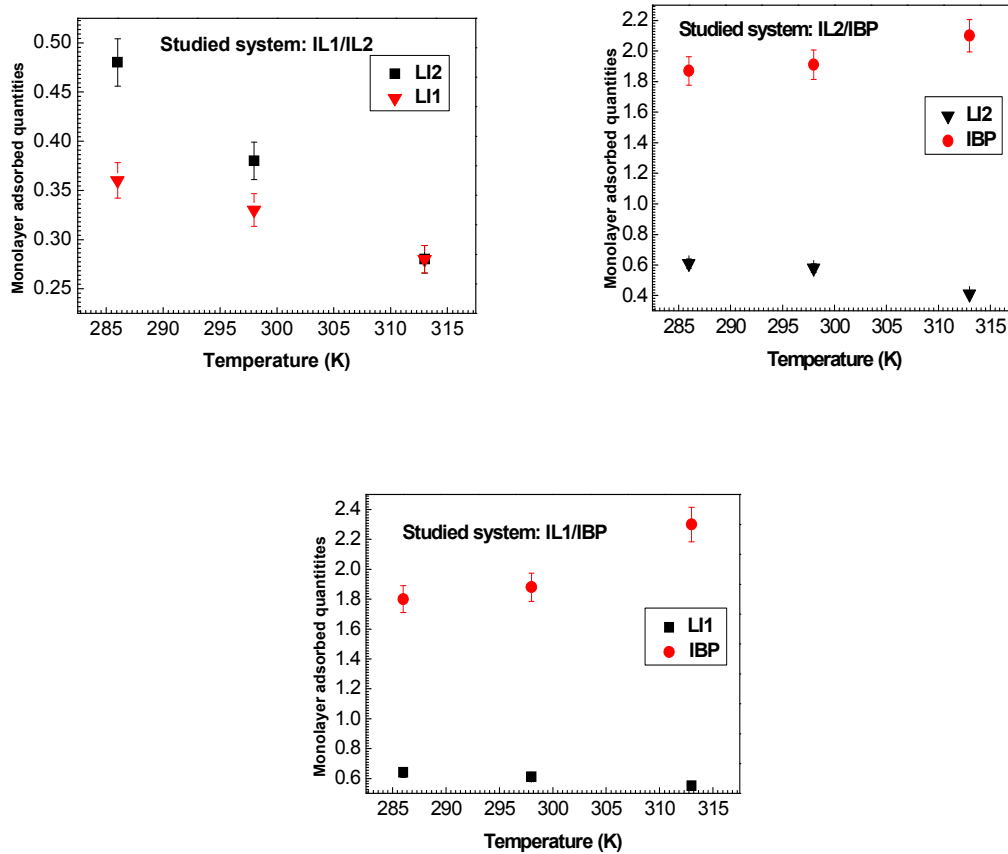
Figure 9: *Evolution of the adsorption energies as function of temperature for the different*

studied systems.
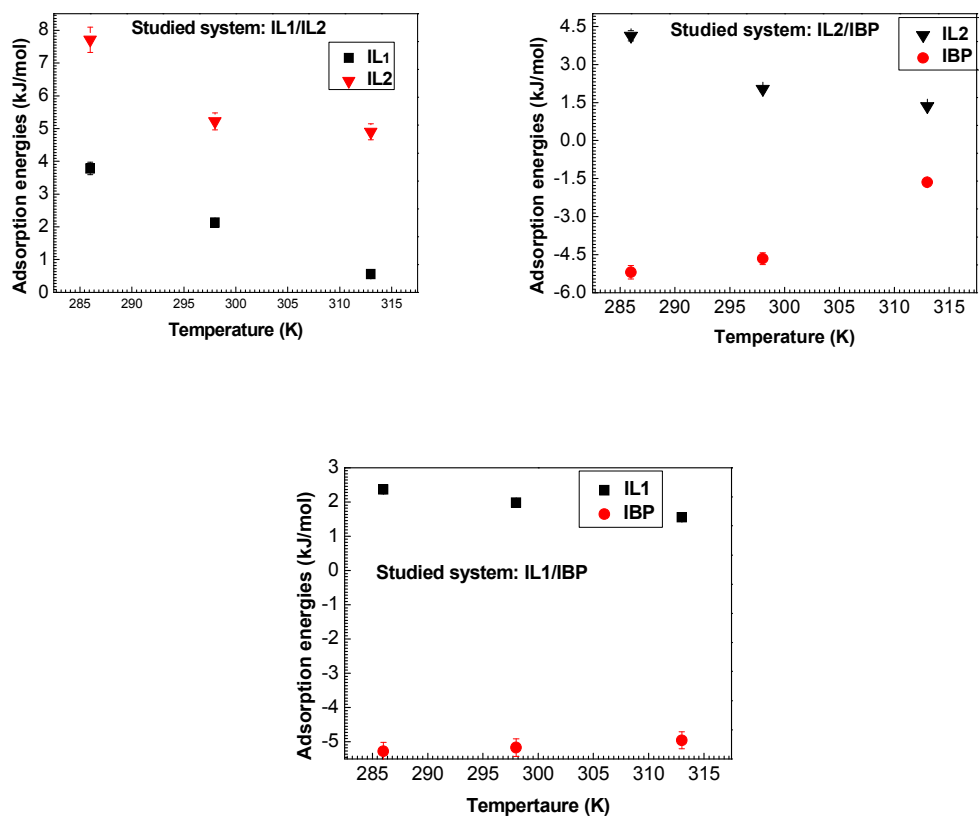
Table 1*: Formula and estimated dimensions of the ILs and IBP.*

Molecular formula	Acronym	Molecular weight (g/mol)	K_{ow} Octanol/Water Partition Coefficient[$]	dimensions of the molecule LxBxT*(nmxnmxnm)
	IL1	258.18	-1.84	1.01×0.76 ×0.75
	IL2	288.18	-2.7	1.12×0.58 ×0.58
	IBP	206.28	3.72	0.87×0.60 ×0.53
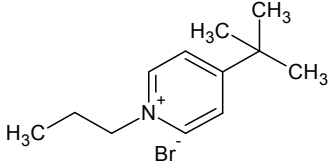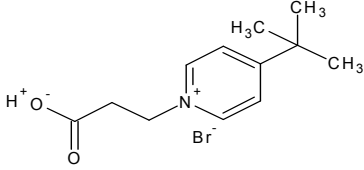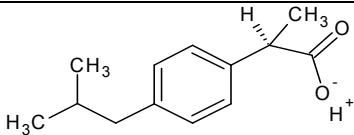
* Length x Breadth x Thickness
[$] Calculated by using Chemsketch software and model of ref [29].

Table 2: *The partition functions and the expressions of the adsorbed quantities of the six*

proposed models.

Model number	Partition function of each model of one receptor site	Expression of each model
Model 1	$z_{gcj} = 1 + e^{\beta(\varepsilon_j + \mu_j)}$ **(Eq 11)**	$Q_{a_j} = \dfrac{n_j N_{M_j}}{1 + \left(\dfrac{(c_{1/2})_j}{c_j} \right)^{n_j}}$ **(Eq 17)**
Model 2	$z_{gcj} = 1 + e^{\beta(\varepsilon_j + \mu_j)}$	$Q_{a_j} = \dfrac{N_{M_j}}{1 + \left(\dfrac{(c_{1/2})_j}{c_j} \right)}$ **(Eq 18)**
Model 3	$z_{gc} = 1 + e^{\beta(\varepsilon_1 + \mu_1)} + e^{\beta(\varepsilon_2 + \mu_2)}$ **(Eq 21)**	$Q_{aj} = \dfrac{n_j N_M \left(\dfrac{c_j}{c_{0j}} \right)^{n_j}}{1 + \left(\dfrac{c_1}{c_{01}} \right)^{n_1} + \left(\dfrac{c_2}{c_{02}} \right)^{n_2}}$ **(Eq 22)**
Model 4	$z_{gc} = 1 + e^{\beta(\varepsilon_1 + \mu_1)} + e^{\beta(\varepsilon_2 + \mu_2)}$	$Q_{aj} = \dfrac{N_M \left(\dfrac{cj}{c_{0j}} \right)}{1 + \left(\dfrac{c_1}{c_{01}} \right) + \left(\dfrac{c_2}{c_{02}} \right)}$ **(Eq 23)**
Model 5	$z_{gc} = 1 + e^{\beta(\varepsilon_1 + \mu_1)} + e^{\beta(\varepsilon_2 + \mu_2)} + e^{\beta(\varepsilon_1 + \varepsilon_2 + \mu_1 + \mu_2)}$ **(Eq 25)**	$Q_{aj} = n_j N_M \dfrac{\left(\dfrac{cj}{c_{0j}} \right)^{nj} + \left(\dfrac{c_1}{c_{01}} \right)^{n_1} \left(\dfrac{c_2}{c_{02}} \right)^{n_2}}{1 + \left(\dfrac{c_1}{c_{01}} \right)^{n_1} + \left(\dfrac{c_2}{c_{02}} \right)^{n_2} + \left(\dfrac{c_1}{c_{01}} \right)^{n_1} \left(\dfrac{c_2}{c_{02}} \right)^{n_2}}$ **(Eq 26)**
Model 6	$z_{gc} = 1 + e^{\beta(\varepsilon_1 + \mu_1)} + e^{\beta(\varepsilon_2 + \mu_2)} + e^{\beta(\varepsilon_1 + \varepsilon_2 + \mu_1 + \mu_2)}$	$Q_{aj} = N_M \dfrac{\left(\dfrac{cj}{c_{0j}} \right) + \left(\dfrac{c_1}{c_{01}} \right) \left(\dfrac{c_2}{c_{02}} \right)}{1 + \left(\dfrac{c_1}{c_{01}} \right) + \left(\dfrac{c_2}{c_{02}} \right) + \left(\dfrac{c_1}{c_{01}} \right) \left(\dfrac{c_2}{c_{02}} \right)}$ **(Eq 27)**

Table 3: Values of the R^2 determination coefficients calculated by using the proposed model i (referred to M i, where i is in the range [1-6]) for three studied binary systems at different temperatures and at r=1.

T(K)	IL1(IL1/IL2) 286	IL1(IL1/IL2) 298	IL1(IL1/IL2) 313	IL2(IL1/IL2) 286	IL2(IL1/IL2) 298	IL2(IL1/IL2) 313
M 1	0.975	0.979	0.985	0.981	0.991	0.992
M 2	0.972	0.974	0.979	0.980	0.981	0.972
M 3	**0.984**	**0.996**	**0.995**	**0.992**	**0.998**	**0.999**
M 4	0.971	0.984	0.982	0.989	0.981	0.989
M 5	0.975	0.979	0.984	0.982	0.991	0.992
M 6	0.983	0.995	0.980	0.991	0.994	0.996

	IL2(IL2/IBP)	IL2(IL2/IBP)	IL2(IL2/IBP)	IBP(IL2/IBP)	IBP(IL2/IBP)	IBP(IL2/IBP)
M 1	0.975	0.979	0.982	0.982	0.977	0.971
M 2	0.971	0.978	0.971	0.980	0.973	0.970
M 3	**0.995**	**0.990**	**0.992**	**0.998**	**0.985**	**0.981**
M 4	0.981	0.987	0.988	0.986	0.982	0.972
M 5	0.991	0.989	0.990	0.984	0.981	0.972
M 6	0.973	0.985	0.977	0.971	0.984	0.976

	IL1(IL1/IBP)	IL1(IL1/IBP)	IL1(IL1/IBP)	IBP(IL1/IBP)	IBP(IL1/IBP)	IBP(IL1/IBP)
M 1	0.989	0.976	0.979	0.979	0.992	0.980
M 2	0.975	0.977	0.970	0.977	0.991	0.972
M 3	**0.999**	**0.996**	**0.979**	**0.989**	**0.997**	**0.980**
M 4	0.971	0.974	0.972	0.977	0.981	0.978
M 5	0.985	0.989	0.975	0.982	0.991	0.972
M 6	0.973	0.975	0.973	0.981	0.984	0.976

M: model

Table 4*: Values of RMSE calculated by using the proposed model i (referred to M i, where i is in the range [1-6]) for the three studied binary systems at different temperatures and at r=1.*

T(K)	IL1(IL1/IL2) 286	IL1(IL1/IL2) 298	IL1(IL1/IL2) 313	IL2(IL1/IL2) 286	IL2(IL1/IL2) 298	IL2(IL1/IL2) 313
M 1	0.008	0.025	0.003	0.019	0.007	0.069
M 2	0.018	0.014	0.013	0.017	0.012	0.011
M 3	**0.003**	**0.004**	**0.002**	**0.003**	**0.004**	**0.006**
M 4	0.007	0.024	0.004	0.004	0.009	0.031
M 5	0.009	0.024	0.013	0.039	0.017	0.079
M 6	0.011	0.030	0.029	0.029	0.017	0.029

	IL2(IL2/IBP)	IL2(IL2/IBP)	IL2(IL2/IBP)	IBP(IL2/IBP)	IBP(IL2/IBP)	IBP(IL2/IBP)
M 1	0.007	0.015	0.008	0.089	0.015	0.049
M 2	0.011	0.024	0.013	0.027	0.014	0.014
M 3	**0.002**	**0.003**	**0.003**	**0.004**	**0.005**	**0.007**
M 4	0.017	0.014	0.009	0.009	0.008	0.041
M 5	0.029	0.034	0.073	0.049	0.027	0.029
M 6	0.071	0.040	0.039	0.019	0.077	0.049

	IL1(IL1/IBP)	IL1(IL1/IBP)	IL1(IL1/IBP)	IBP(IL1/IBP)	IBP(IL1/IBP)	IBP(IL1/IBP)
M 1	0.027	0.015	0.038	0.049	0.045	0.029
M 2	0.071	0.034	0.023	0.017	0.044	0.024
M 3	**0.004**	**0.005**	**0.002**	**0.006**	**0.007**	**0.009**
M 4	0.077	0.074	0.029	0.019	0.018	0.051
M 5	0.019	0.037	0.075	0.040	0.020	0.024
M 6	0.081	0.043	0.033	0.018	0.057	0.059

M : model

Table 5: *Different values of the molecular interaction energies of the three studied system at*

T=298 K.

Studied system	Misfit (kJ/mol)	Hydrogen-Bond (kJ/mol)	Van der Waals (kJ/mol)	Misfit (kcal/mol)	Hydrogen-Bond (kJ/mol)	Van der Waals (kJ/mol)
IL1/IL2/carbon		**IL1**			**IL2**	
	10.07	-0.01672	-59.8158	15.257	-26.2504	-57.0988
IL1/IBP/carbon		**IL1**			**IBP**	
	9.9066	-0.00836	-59.6068	14.212	-19.8132	-54.2146
IL2/IBP/carbon		**IL2**			**IBP**	
	15.2152	-29.0092	-56.5554	14.1702	-21.318	-53.8802

Graphical Abstract
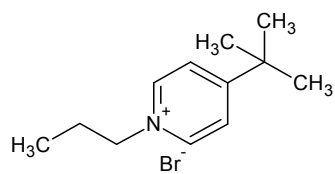
IL1
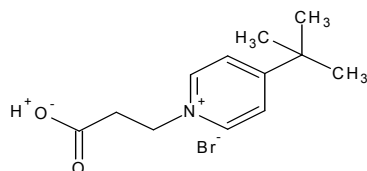
IL2
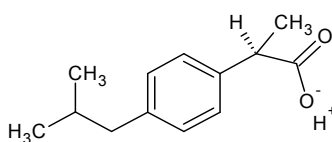
IBP

Chemical structures of IL1, IL2 and IBP.